

Gallium nitride nanorod arrays as low-refractive-index transparent media in the entire visible spectral region

Hung-Ying Chen,¹ Hon-Way Lin,¹ Chen-Ying Wu,¹ Wei-Chun Chen,² Jyh-Shin Chen,²
and Shangjr Gwo^{1,2,*}

¹Department of Physics, National Tsing-Hua University
Hsinchu 300, Taiwan, Republic of China

²Instrument Technology Research Center, National Applied Research Laboratories,
Hsinchu 300, Taiwan, Republic of China

*Corresponding author: gwo@phys.nthu.edu.tw

Abstract: Vertically aligned gallium nitride (GaN) nanorod arrays grown by the catalyst-free, self-organized method based on plasma-assisted molecular-beam epitaxy are shown to behave as subwavelength optical media with low effective refractive indices. In the reflection spectra measured in the entire visible spectral region, strong reflectivity modulations are observed for all nanorod arrays, which are attributed to the effects of Fabry-Pérot microcavities formed within the nanorod arrays by the optically flat air/nanorods and nanorods/substrate interfaces. By analyzing the reflectivity interference fringes, we can quantitatively determine the refractive indices of GaN nanorod arrays as functions of light wavelength. We also propose a model for understanding the optical properties of GaN nanorod arrays in the transparent region. Using this model, good numerical fitting can be achieved for the reflectivity spectra.

©2008 Optical Society of America

OCIS codes: (160.5320) Photorefractive materials; (160.4236) Thin films, optical properties; (160.4236) Nanomaterials; (160.6000) Semiconductor Materials; (300.6550) Spectroscopy, visible; (260.2065) Effective medium theory.

References and links

1. P. B. Clapham and M. C. Hutley, "Reduction of lens reflexion by the 'moth eye' principle," *Nature* **244**, 281–282 (1973).
2. S. J. Wilson and M. C. Hutley, "The optical properties of 'moth eye' antireflection surfaces," *Opt. Acta* **29**, 993–1009 (1982).
3. M. Srinivasarao, "Nano-optics in the biological world: Beetles, butterflies, birds, and moths," *Chem. Rev.* **99**, 1935–1961 (1999).
4. M. E. Motamedi, W. H. Southwell, and W. J. Gunning, "Antireflection surfaces in silicon using binary optics technique," *Appl. Opt.* **31**, 4371–4376 (1992).
5. P. Lalanne and G. M. Morris, "Antireflection behavior of silicon subwavelength periodic structures for visible light," *Nanotechnology* **8**, 53–56 (1997).
6. Y. Kanamori, K. Hane, H. Sai, and H. Yugami, "100 nm period silicon antireflection structures fabricated using a porous alumina membrane mask," *Appl. Phys. Lett.* **78**, 142–143 (2001).
7. D. E. Aspnes, "Optical properties of thin-films," *Thin Solid Films* **89**, 249–262 (1982).
8. D. R. Smith, W. J. Padilla, D. C. Vier, S. C. Nemat-Nasser, and S. Schultz, "Composite medium with simultaneously negative permeability and permittivity," *Phys. Rev. Lett.* **84**, 4184–4187 (2000).
9. D. R. Smith, J. B. Pendry, and M. C. K. Wiltshire, "Metamaterials and negative refractive index," *Science* **305**, 788–792 (2004).
10. J.-Q. Xi, J. K. Kim, and E. F. Schubert, "Silica nanorod-array films with very low refractive indices," *Nano Lett.* **5**, 1385–1387 (2005).
11. J.-Q. Xi, J. K. Kim, E. F. Schubert, D. Ye, T.-M. Lu, and S.-Y. Lin, "Very low-refractive-index optical thin films consisting of an array of SiO₂ nanorods," *Opt. Lett.* **31**, 601–603 (2006).
12. J.-Q. Xi, M. F. Schubert, J. K. Kim, E. F. Schubert, M. Chen, S.-Y. Lin, W. Liu, and J. A. Smart, "Optical thin-film materials with low refractive index for broadband elimination of Fresnel reflection," *Nat. Photonics* **1**, 176–179 (2007).

13. C.-H. Hsu, H.-C. Lo, C.-F. Chen, C. T. Wu, J.-S. Hwang, D. Das, J. Tsai, L.-C. Chen, and K.-H. Chen, "Generally applicable self-masked dry etching technique for nanotip array fabrication," *Nano Lett.* **4**, 471–475 (2004).
14. Y.-F. Huang, S. Chattopadhyay, Y.-J. Jen, C.-Y. Peng, T.-A. Liu, Y.-K. Hsu, C.-L. Pan, H.-C. Lo, C.-H. Hsu, Y.-H. Chang, C.-S. Lee, K.-H. Chen, and L.-C. Chen, "Improved broadband and quasi-omnidirectional anti-reflection properties with biomimetic silicon nanostructures," *Nat. Nanotechnol.* **2**, 770–774 (2007).
15. H.-Y. Chen, H.-W. Lin, C.-H. Shen, and S. Gwo, "Structure and photoluminescence properties of epitaxially oriented GaN nanorods grown on Si (111) by plasma-assisted molecular-beam epitaxy," *Appl. Phys. Lett.* **89**, 243105 (2006), and references therein.
16. E. F. Schubert, *Light-Emitting Diodes, 2nd Edition* (Cambridge University Press, Cambridge, 2006).
17. T. Fujii, Y. Gao, R. Sharma, E. L. Hu, S. P. DenBaars, and S. Nakamura, "Increase in the extraction efficiency of GaN-based light-emitting diodes via surface roughening," *Appl. Phys. Lett.* **84**, 855–857 (2004).
18. T. N. Oder, K. H. Kim, J. Y. Lin, and H. X. Jiang, "III-nitride blue and ultraviolet photonic crystal light emitting diodes," *Appl. Phys. Lett.* **84**, 466–468 (2004).
19. J. J. Wierer, M. R. Krames, J. E. Epler, N. F. Gardner, M. G. Craford, J. R. Wendt, J. A. Simmons, and M. M. Sigalas, "InGaN/GaN quantum-well heterostructure light-emitting diodes employing photonic crystal structures," *Appl. Phys. Lett.* **84**, 3885–3887 (2004).
20. A. David, T. Fujii, R. Sharma, K. McGroddy, S. Nakamura, S. P. DenBaars, E. L. Hu, C. Weisbuch, and H. Benisty, "Photonic-crystal GaN light-emitting diodes with tailored guided modes distribution," *Appl. Phys. Lett.* **88**, 061124 (2006).
21. J. Y. Kim, T. Gessmann, E. F. Schubert, J.-Q. Xi, H. Luo, J. Cho, C. Sone, and Y. Park, "GaInN light-emitting diode with conductive omnidirectional reflector having a low-refractive-index indium-tin oxide layer," *Appl. Phys. Lett.* **88**, 013501 (2006).
22. J. Zhong, H. Chen, G. Saraf, Y. Lu, C. K. Choi, J. J. Song, D. M. Mackie, and H. Shen, "Integrated ZnO nanotips on GaN light emitting diodes for enhanced emission efficiency," *Appl. Phys. Lett.* **90**, 203515 (2007).
23. H.-M. Kim, T. W. Kang, and K. S. Chung, "Nanoscale ultraviolet-light-emitting diodes using wide-bandgap gallium nitride nanorods," *Adv. Mater.* **15**, 567–569 (2003).
24. H.-M. Kim, Y.-H. Cho, H. Lee, S. I. Kim, S. R. Ryu, D. Y. Kim, T. W. Kang, and K. S. Chung, "High-brightness light emitting diodes using dislocation-free indium gallium nitride/gallium nitride multiquantum-well nanorod arrays," *Nano Lett.* **4**, 1059–1062 (2004).
25. A. Kikuchi, M. Kawai, M. Tada, and K. Kishino, "InGaN/GaN multiple quantum disk nanocolumn light-emitting diodes grown on (111) Si substrate," *Jpn. J. Appl. Phys.* **43**, L1524–L1526 (2004).
26. A. Kikuchi, M. Tada, K. Miwa, and K. Kishino, "Growth and characterization of InGaN/GaN nanocolumn LED," *Proc. SPIE* **6129**, 612905 (2006).
27. K. Kishino, A. Kikuchi, H. Sekiguchi, and S. Ishizawa, "InGaN/GaN nanocolumn LEDs emitting from blue to red," *Proc. SPIE* **6473**, 64730T (2007).
28. G. Yu, G. Wang, H. Ishikawa, M. Umeno, T. Soga, T. Egawa, J. Watanabe, and T. Jimbo, "Optical properties of wurtzite structure GaN on sapphire around fundamental absorption edge (0.78–4.77 eV) by spectroscopic ellipsometry and the optical transmission method," *Appl. Phys. Lett.* **70** 3209–3211 (1997); the refractive index n was found to follow the Sellmeier-type dispersion relationship $n^2(\lambda) = 2.27^2 + 304.7^2/(\lambda^2 - 294.0^2)$ with the incident photon energy below the fundamental band edge of wurtzite GaN.
29. T. Kawashima, H. Yoshikawa, S. Adachi, S. Fuke, and K. Ohtsuka, "Optical properties of hexagonal GaN," *J. Appl. Phys.* **82**, 3528–3535 (1997).
30. H. C. van de Hulst, *Light Scattering by Small Particles* (Dover Publications, New York, 1981).

1. Introduction

The ultimate goal of controlling the properties of optical media is to manipulate their refractive indices, which can alter their behaviors in light reflection, refraction, diffraction, and interference. For semiconductors, the problem of surface reflection is particularly severe because semiconductors have very high values of refractive index in the visible and near infrared spectral regions. For example, in the near-infrared region, the reflection loss of silicon in air is ~30% at normal incidence. Thus, achieving a way to reduce the reflection loss would be of interest for Si-based solar-cell and optoelectronic device applications. At present, there are some possibilities to overcome this problem. For instance, nanostructured periodic or aperiodic surfaces with feature sizes less than the light wavelength have been known to exhibit the antireflective effects of zero-order gratings (also known as the moth-eye effects) [1-6].

Alternatively, there are other approaches utilizing the optical properties of nanocomposite materials. In such type of materials, if the feature sizes of the embedded nanostructures in a composite material are significantly smaller than the wavelength of incident light, the

embedded nanostructures would not be resolved by the light and the composite material behaves as an effective medium with its optical properties interpolated between those of composing materials [7]. Therefore, by varying the filling factor (volume fraction) of the embedded nanostructures, it is possible to control the effective refractive index and engineer new optical materials previously unavailable in nature. Recently, the availability of new nanofabrication technologies and synthesis routes of nanostructured materials have made it possible to consider various artificial subwavelength optical media [8-14]. However, most of the reported subwavelength antireflective structures are made from silicon using lithographic methods [4-6] or other means (e.g., self-masked dry etching technique, see Refs. [13,14]). Here, we demonstrate that vertically aligned gallium nitride (GaN) nanorod arrays prepared by a catalyst-free, self-organized epitaxial growth method [15] can be used as subwavelength structured optical media with low effective refractive indices in the entire visible spectral region.

Recently, GaN-based light-emitting diodes (LEDs) and lasers have become the major choice for devices operating in the short wavelength range because of the ambipolar dopability of GaN [16]. One of the remaining challenges for improving GaN-based LEDs is to reduce their optical losses, originating from the high refractive index of GaN (~2.5). For example, to realize general solid-state lighting or full-color display using high-efficiency GaN-based LEDs, it is important to enhance their light extraction efficiency, which is limited by the loss of total internal reflection. For an air/GaN planar interface, the critical angle for total internal reflection is only ~24° and only about 4% ($\approx 1/(4n^2)$, where n is the refractive index of GaN) of the emitting light can escape from the GaN region. There have been extensive ongoing research efforts to improve the light extraction efficiency of GaN-based LEDs, such as surface subwavelength texturing [17] or incorporation of photonic crystals in the LED structures [18-20]. However, these methods might not be practical for large-scale applications due to their complicate and costly lithographic processes. More recently, a new approach has been proposed to enhance light extraction efficiency by using transparent, conductive indium-tin oxide [21] and ZnO [22] nanorod arrays with low effective refractive indices. In comparison with these nanorod materials, GaN nanorod arrays can be doped to be both n - and p -type, and have the same physical and thermal properties as the bulk GaN crystal, making them more suitable and durable for high-power GaN-based optoelectronic applications. Furthermore, it has been shown that incorporation of active regions within the GaN nanorods is a viable approach to fabricate GaN-nanorod-based LEDs [23-27]. The aforementioned characteristics of GaN nanorod arrays make them particularly interesting for future GaN-based light emitting applications as low-refractive-index optical media.

2. Sample growth and optical measurements

Vertically aligned, wurtzite GaN nanorod arrays studied here were grown on 3-inch Si(111) wafers by plasma-assisted molecular-beam epitaxy (PA-MBE). The details of growth process can be found elsewhere [15]. The grown GaN nanorod arrays have been confirmed to be single crystalline and epitaxially oriented with the epitaxial relationship of $\langle 2\bar{1}\bar{1}0 \rangle_{\text{GaN}} \parallel \langle \bar{1}10 \rangle_{\text{Si}}$ and $\langle 1\bar{1}00 \rangle_{\text{GaN}} \parallel \langle 11\bar{2} \rangle_{\text{Si}}$. And, the GaN nanorods are nitrogen-polar with the axial direction pointed to the $-c$ -axis ($[000\bar{1}]$ direction). The reflectivity spectra were measured using a Perkin-Elmer Lambda 900 spectrophotometer equipped with a tungsten lamp and an integrating sphere/photomultiplier tube for collecting the reflected light. This system was calibrated by a standard aluminum mirror from National Physical Laboratory (NPL, U.K.).

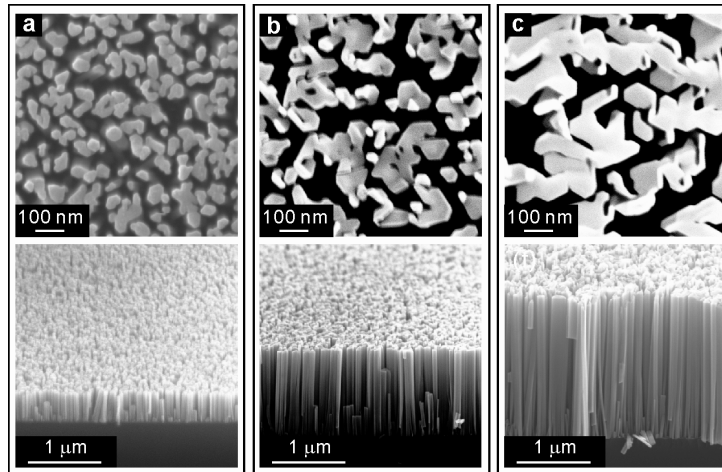


Fig. 1. FE-SEM images of the vertically aligned GaN nanorod arrays grown on Si(111) by PA-MBE. Plan view (upper panels) and cross-sectional (lower panels) view of (a) 0.4 μm , (b) 1.2 μm , and (c) 2 μm GaN nanorod arrays.

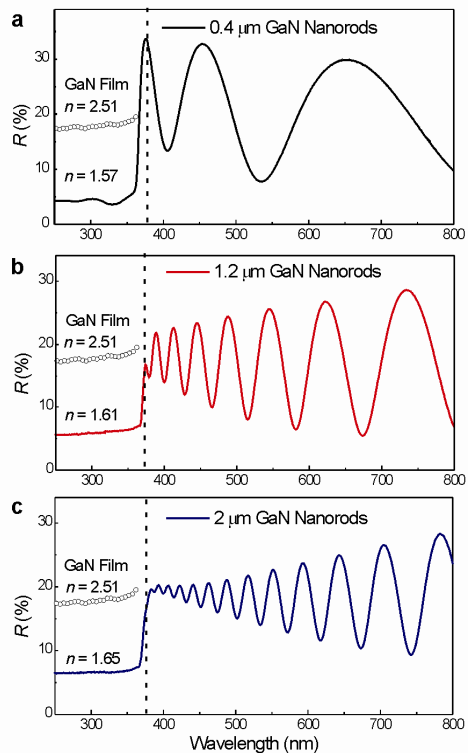


Fig. 2. Normal-incidence reflectivity spectra of vertically-aligned GaN nanorod arrays. The dashed line labels the incident photon energy that corresponds to the GaN band gap energy. To the left of the dashed line is the opaque region, and to the right of the dashed line is the transparent region. The dotted curves in the opaque region are the reflectivities of GaN epilayers measured with the same set-up.

3. Results and discussion

Figure 1 shows the field-emission scanning electron microscope (FE-SEM) images in the plan and tilted views of GaN nanorods with different plasma-assisted molecular-beam epitaxy (PA-MBE) growth times, corresponding to the rod lengths of 0.4 μm , 1.2 μm , and 2 μm , respectively. In the tilted view of GaN nanorods, no significant lateral growth of individual nanorods can be found. We also find that the mean diameter and aerial density of GaN nanorods depend on the growth temperature and III/V ratio, whereas the nanorod height mainly depends on the growth time. Analyzing from the FE-SEM images, independent of the nanorod length, the PA-MBE-grown GaN nanorods exhibit a uniform mean diameter of ~ 40 nm (standard deviation ~ 20 nm) and an aerial density of $\sim 5 \times 10^{10} \text{ cm}^{-2}$. Moreover, the height of GaN nanorods appears to be quite uniform, forming an optically flat interface with the ambient air. Thus, the aspect ratio of nanorods can be simply controlled by growth time and the percentage of aerial coverage in the plan view can be regarded as the volume fraction occupied by the GaN nanorods. With increasing growth time (longer nanorod length), individual nanorods gradually coalesce into nanorod bundles on the top region of the GaN nanorod arrays, which can be clearly seen in the tilted-view FE-SEM images. Although the coalescence phenomenon becomes serious for the case of long GaN nanorods, the percentage of coverage are $50 \pm 5\%$ for all samples. Here, the percentage of nanorod coverage is estimated by analyzing the contrast distributions [gray-scale histograms, ranging from 0 (white) to 255 (black)] in the plan-view FE-SEM images. A threshold gray level, corresponding to the nanorod edges, is selected first. And, the shaded area from zero to the threshold level in the histogram is used to determine the total number of image pixels that GaN nanorods occupy. Therefore, the percentage of coverage can be determined by the ratio of nanorod-occupied pixels to the total pixels in the FE-SEM image. The uncertainty of measurement exists due to the limited image resolution (i.e., boundary sharpness) and limited gray levels.

Figure 2 shows the normal-incidence reflectivity spectra in the near-ultraviolet (UV) and visible regions from three GaN nanorod arrays, corresponding to rod lengths of 0.4 μm , 1.2 μm , and 2 μm , respectively. As can be clearly seen in the spectra, when the incident photon energy is larger than the direct band gap energy of GaN (3.4 eV; the wavelength of incident light in air $\lambda < 365$ nm), flat and featureless reflectivity spectra are observed. On the contrary, strongly modulated reflectivity spectra are measured when the incident photon energy is below the band gap energy of GaN (in the transparent region). In Fig. 2, the observed reflectivity fringe strongly depends on the rod length of nanorod arrays, suggesting that optical interference might be responsible for the observed reflectivity modulation in the transparent region. Indeed, as will be shown in the following discussion, this phenomenon can be attributed to the effects of Fabry-Pérot microcavities formed within the nanorod arrays by the optically flat air/nanorods and nanorods/substrate interfaces.

First of all, we discuss the results of reflectivity measurements in the opaque region, where the incident light can only penetrate a limited depth of GaN nanorod arrays near the air interface. In this probing depth, the effective refractive index can be expressed as a complex number $N_{\text{eff}} = n_{\text{eff}} + ik_{\text{eff}}$ and the imaginary part k_{eff} is a nonzero real number, which can be used to determine the light absorption coefficient ($\alpha = 4\pi k_{\text{eff}} / \lambda$). For GaN, the near-UV light penetration depth is smaller than 100 nm [28]. Thus, the single reflection at the interface between air and GaN nanorod array can be approximated to the total film reflection. By applying the Fresnel equation and $n_{\text{air}} = 1.0$, the normal-incidence reflectivity

$$R = |r|^2 = \frac{(n_{\text{eff}} - 1)^2 + k_{\text{eff}}^2}{(n_{\text{eff}} + 1)^2 + k_{\text{eff}}^2} \approx \frac{(n_{\text{eff}} - 1)^2}{(n_{\text{eff}} + 1)^2}$$

for photon energy just above the fundamental absorption edge ($k_{\text{eff}}^2 \ll 1$; for bulk GaN, $n \approx 2.5$ and $k \approx 0.3$ in the near-UV range [29]). As can be seen from Fig. 2, above the band gap energy ($\lambda < 365$ nm), the reflectivity is $\sim 5.5\%$ for 1.2 μm GaN nanorods. Therefore, the effective reflective index can be estimated to be 1.61. The

effective reflective indices of the other nanorod array samples determined by this method show similar figures, independent of the nanorod length.

By applying the effective medium theory for composite materials, the volume fraction of GaN nanorods and the refractive index of bulk GaN can also be used to determine the effective refractive index of GaN nanorod arrays. In the Bruggemann effective medium approximation [7, 21], the following expression holds for the effective refractive index of GaN nanorod arrays

$$f_{\text{GaN}} \frac{n_{\text{GaN}}^2 - n_{\text{eff}}^2}{n_{\text{GaN}}^2 + 2n_{\text{eff}}^2} + (1 - f_{\text{GaN}}) \frac{n_{\text{air}}^2 - n_{\text{eff}}^2}{n_{\text{air}}^2 + 2n_{\text{eff}}^2} = 0, \quad (1)$$

where n_{eff} is the effective refractive index of GaN nanorod array and f_{GaN} is the volume fraction of GaN nanorods. The volume fraction of GaN nanorods is close to the percentage of nanorod aerial coverage, which is ~50% for all nanorod samples studied here. Thus, the effective refractive index can be calculated to be ~1.70 using the parameters of $f_{\text{GaN}} = 0.5$, $n_{\text{GaN}} = 2.5$, and $n_{\text{air}} = 1.0$. This value is in good agreement with that obtained by the reflectivity measurements, indicating that the Bruggemann effective medium approximation works well for this composite material system in the opaque region.

In the transparent region, the optical media is non-absorbing and the imaginary part of the effective refractive index is negligible. However, the analysis of reflectivity spectrum is more complex due to the effects of multiple reflections within the nanorod array. The amplitude reflection coefficient at normal incidence can also be described by the Fresnel equation. For the present case, the amplitude reflection coefficient of air/nanorods interface is $r_1 = (1 - n_{\text{eff}})/(1 + n_{\text{eff}})$; and the amplitude reflection coefficient of nanorods/substrate interface is $r_2 = (n_{\text{eff}} - n_{\text{Si}})/(n_{\text{eff}} + n_{\text{Si}})$, where n_{Si} is the refractive index of Si substrate. Therefore, the amplitude reflection coefficient of the total reflected light (r) can be obtained by summing up an infinite series of partial reflected waves after multiple reflections within the nanorod-array microcavity. The resulting reflectivity is

$$R = |r|^2 = \left| \frac{r_1 + r_2 e^{i\varphi}}{1 + r_1 r_2 e^{i\varphi}} \right|^2, \quad (2)$$

where φ is the phase difference due to the optical path within the microcavity and $\varphi = 4\pi n_{\text{eff}} d / \lambda$ (d is the length of GaN nanorods and n_{eff} is the effective refractive index of GaN nanorod array).

The measured reflectivity spectra in the transparent region are superimposed with strong interference fringes (Fig. 2) of partial reflected waves after multiple reflections between the interfaces of air/nanorods and nanorods/substrate. The condition for observing the interference extrema (maximum or minimum) in a normal-incidence reflectivity spectrum is $\varphi = 4\pi n_{\text{eff}} d / \lambda_l = (2m + l)\pi$, where m is a fixed integer, corresponding to the anti-node number of the standing wave in nanorod-array microcavity at $l = 0$, and l is an even integer for reflectivity maxima and an odd integer for reflectivity minima. At the specific wavelength positions (λ_l) in the reflectivity spectrum, the extremum reflectivity occurs due to totally constructive or destructive interference. We can rewrite this condition as

$$\frac{l}{2} = \frac{2n_{\text{eff}} d}{\lambda_l} - m, l = 0, 1, 2, \dots \quad (3)$$

As indicated in Eq. (3), if n_{eff} is independent of λ , $2d/\lambda_l$ and $l/2$ should have a linear relationship. In practice, the reflective index of GaN is actually quite close to a constant in the long wavelength region. Hence, the linear relationship can be applied in this region for determination of m value. By using the known values of d and m , we then can quantitatively

determine the effective refractive indices of GaN nanorod arrays as functions of incident light wavelength λ_l with the simple relation of

$$n_{\text{eff}} = \frac{(2m+l)\lambda_l}{4d}. \quad (4)$$

In order to validate the technique that we would like utilize for finding the dispersion relationships of nanorod-array effective refractive indices, we apply it first to a high-quality GaN bulk film (970 nm in thickness, as determined by FE-SEM cross-sectional thickness measurement) grown on a Si(111) substrate by PA-MBE. Figure 3 shows the reflectivity spectra of GaN bulk film and bare Si(111) substrate and the determined dispersion relationship of refractive index for this GaN film. As can be seen from Fig. 3(a), the maxima of GaN film reflectivity spectrum are enveloped by the reflectivity spectrum of Si(111) substrate, indicating the absorption coefficient is negligible in the transparent region. In Fig. 3(b), the data points correspond to the interference extrema obtained from the interference fringe in the reflectivity spectrum of GaN film. And, the solid line is a linear fit in the long wavelength region, where the refractive index of GaN is close to a constant. In the short wavelength region, the data points show an upward deviation from the straight line due to the refractive index dispersion of GaN. Using the present technique, the m value (vertical-axis intercept) of the observed interference fringe can be extrapolated to be 7. It should be noted that this approach is rather robust since the value of m is restricted to an integer. For instance, at $l = 0$, the linear fits of $m = 6$ or 8 would yield $n_{\text{GaN}} = \sim 2.0$ and ~ 2.7 , significantly different from the known value of n_{GaN} in the visible light region (~ 2.3 – 2.5). Using the values of $m = 7$ and $d = 970$ nm, the dispersion relationship can then be obtained by substituting $l = 0, 1, 2, 3$, etc. in Eq. (4). As a comparison, the solid line shown in Fig. 3(c) is the Sellmeier-type dispersion relationship of GaN-bulk-film refractive index determined by the techniques of spectroscopic ellipsometry and optical transmission [28]. The dispersion relationship determined by our method shows a perfect match with the previously reported relationship.

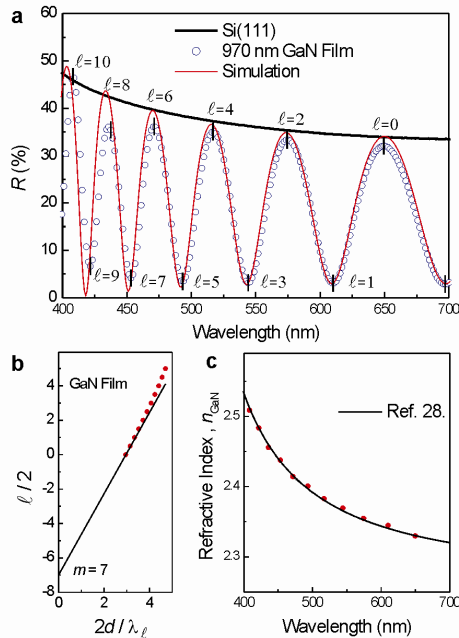


Fig. 3. Dispersion relationship of GaN-bulk-film refractive index determined by reflectivity spectroscopy in the transparent region. The result obtained by our method agrees well with that measured by spectroscopic ellipsometry and optical transmission in Ref. [28].

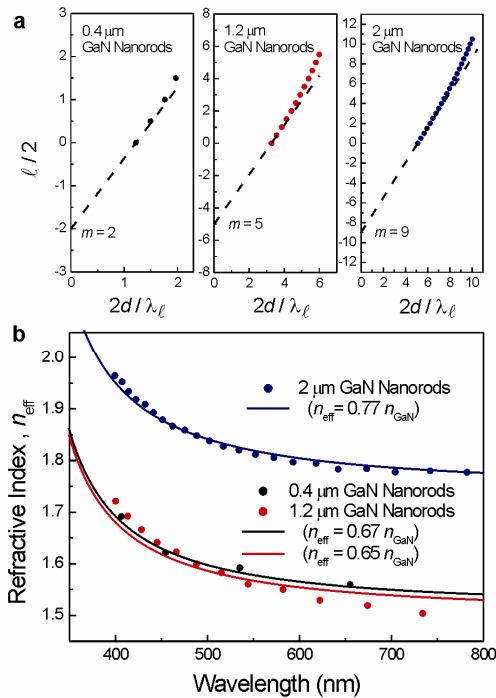


Fig. 4. Determination of effective refractive index dispersion curves of GaN nanorod array. (a) The relations of $2d/\lambda_l$ and $l/2$ for the nanorod-array samples. The dashed lines are linear fits (in the long wavelength region) with integer intercepts on the vertical axis. (b) The effective refractive index dispersion curves obtained from the interference fringes of reflectivity spectra for all GaN nanorod-array samples. The solid lines are the dispersion curves obtained by multiplying the dispersion curve of GaN-bulk-film refractive index [n_{GaN} , as shown in Fig. 3(c)] with constant numbers.

Figure 4(a) shows the relations between $2d/\lambda_l$ and $l/2$ for three cases of GaN nanorod arrays. For those interference extrema in the long wavelength region (small l), linear fits with integer intercepts on the vertical axis can be obtained, as shown as the dashed lines in Fig. 4(a). The intercept on the vertical axis corresponds to the anti-node number m at λ_0 ($l = 0$). Consequently, $n_{\text{eff}}(\lambda_l)$ can be determined from substituting known values of m and d into Eq. (4). In Fig. 4(b), the determined $n_{\text{eff}}(\lambda)$ relationships nearly overlap for the cases of 0.4 μm and 1.2 μm GaN nanorod arrays. In the effective medium theory, the effective refractive index $n_{\text{eff}}(\lambda)$ depends on the material distribution of composite materials. For these two cases, the GaN nanorods are uniformly distributed without significant lateral growth and coalescence; thus, a similar $n_{\text{eff}}(\lambda)$ of GaN nanorod arrays with different nanorod heights can be expected. The important finding in this analysis is that the effective refractive indices of nanorod arrays in the transparent region can be approximated to the entire dispersion relationship of GaN-bulk-film refractive index by multiplying with a constant of ~ 0.65 . This value is also in agreement with that obtained earlier for the opaque region. By contrast, a gradient refractive index medium can be formed for the long GaN nanorod arrays due to the severe nanorod coalescence behavior with increasing growth time. Figure 5 shows an FE-SEM image of 2- μm -long GaN nanorod array near the sample cleavage edge, where the nanorod bundling phenomenon can be seen more clearly. These nanorod bundles consist of coalesced nanorods on the top region and separated nanorods in the bottom part. Therefore, the nanorod bundles on the top region can be considered as bulk GaN with $n \approx 2.5$. As a result, nanorod bundles formed by long GaN nanorods correspond to optical media with vertically gradient refractive

indices. Gradient refractive index structures have long been applied for antireflection coatings. Recently, Si nanotip (core-like rod) arrays have also been found to show the similar properties [14]. The main point of using gradient refractive index structures is that the reflection at interface can be reduced by gradually changing the difference in refractive index from two light propagating regions. However, in our case, although the long GaN nanorod array has a vertically gradient refractive index, the highest refractive index layer occurs on the top interface with the ambient air. This up-side-down feature would actually result in higher reflection from the air/nanorods interface compared with that of short GaN nanorod arrays. Therefore, the significant deviation of 2- μm GaN nanorod array from the dispersion relationship of short GaN nanorod arrays should be due to the striking nanorod coalescence behavior near the top surface. In the transparent region, light would not just “encounter” the near-surface region but also pass through the entire medium. Thus, the effective refractive index depends not only on the lateral coverage but also on the vertical profile of GaN nanorod arrays. In the case of long nanorod arrays showing significance nanorod bundling, a straightforward interpretation using a uniform effective medium approximation, such as the Bruggemann approximation, would not be appropriate to describe their optical properties in the transparent region. For example, according to the Bruggemann approximation, the volume fraction of GaN nanorods should be 65% to account for the measured n_{eff} of 2- μm GaN nanorod array. This value is very different from the SEM result ($50\pm 5\%$).

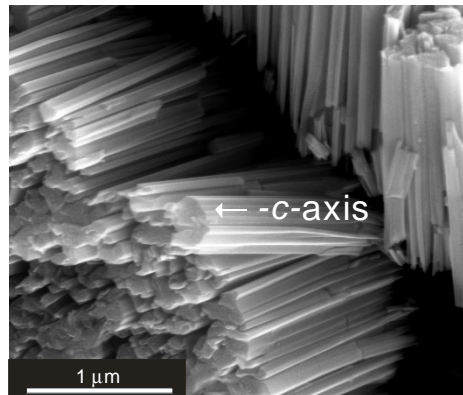


Fig. 5. FE-SEM image of 2- μm -long GaN nanorod array near the sample cleavage edge. The arrow directs toward the top region of vertically aligned nanorod array.

In addition the interference fringes, there are also two conspicuous features in the reflectivity spectra measured for the nanorod arrays. In principle, at the wavelengths of maximum reflectivity of a perfectly transparent film sandwiched between the air and substrate, the film reflectivity should be equal to the reflectivity of the bare substrate, i.e., $|r|^2 = |(1 - n_s)/(1 + n_s)|^2$ [one example is shown in Fig. 3(a)]. This result can be derived directly from Eq. (2) using the interference condition of $e^{i\phi} = 1$ and $k = 0$. However, the maximum reflectivities of nanorod arrays follow a decaying envelope with decreasing wavelengths. Therefore, the k_{eff} values of GaN nanorod arrays in the transparent region are small but not negligible. Also, the k_{eff} values might have strong wavelength dependence, resulting from the light scattering within the subwavelength nanorod media and at their interfaces. For example, in the case of Rayleigh scattering by small dielectric spheres in the long wavelength limit, the scattering cross section is proportional to λ^{-4} . And, for the case of circular cylinders in the long wavelength limit, which is more appropriate to our case, the scattering cross section is proportional to λ^{-3} [30]. Furthermore, in the transparent region, the

reflectivities of all measured GaN nanorod arrays appear to converge toward that of GaN bulk film at the absorption edge. Based on these features, we propose that the total amplitude coefficient reflected from the nanorod array can be modeled using the following equation

$$r = r_1 + \left[(1 - r_1^2) r_2 e^{i\varphi} - (1 - r_1^2) r_1 r_2^2 e^{i2\varphi} + (1 - r_1^2) r_1^2 r_2^3 e^{i3\varphi} - \dots \right], \quad (5)$$

where the first term comes from the reflection of the air/nanorods interface and the rest of the terms come from the multiply reflected waves, which traverse the entire nanorod effective medium. For the reflection coefficients at interfaces, we apply the known n_{GaN} dispersion relationship of bulk GaN [shown in Fig. 3(c)]. And, for the phase terms, we apply the measured n_{eff} and include the extra correction of $(4\pi/\lambda)ik_{\text{eff}}d$, where an identical k_{eff} dispersion relationship of $9000/\lambda^2$ for all nanorod arrays is assumed. The λ^{-2} dependence of k_{eff} indicates that the loss mechanism should be proportion to λ^{-3} . Using this model, all measured reflectivities of nanorod arrays can converge to that of bulk GaN film at short wavelengths. Figure 6 shows the simulation results of measured reflectivity spectra from GaN nanorod arrays. The solid lines are the fits based on Eq. (5). Excellent simulation results can be obtained for all three samples, demonstrating the validity of the present model.

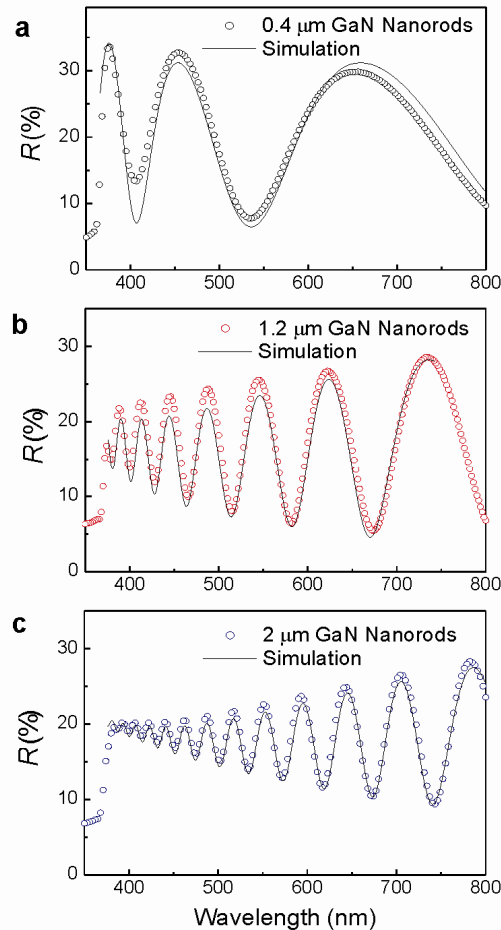


Fig. 6. Comparison of simulated and experimental reflectivity spectra. The simulation results correspond to (a) 0.4 μm , (b) 1.2 μm , and (c) 2 μm GaN nanorods, respectively. Color dots represent the data point and the solid lines are the simulation results using the model described in the text.

4. Conclusions

We have demonstrated that vertically aligned GaN nanorod arrays grown by PA-MBE can act as subwavelength low-refractive-index optical media in both transparent and opaque regions. By using the method of reflectivity spectroscopy in the visible spectral region, we can clearly observe the effects of nanorod-array microcavities formed between the optically flat air/nanorods and nanorods/substrate interfaces realized by the PA-MBE technique. We have also found a simple and reliable technique for analyzing the observed interference fringes in the reflectivity spectra. By using this generally applicable method, we can derive the effective refractive indices for various nanorod arrays, which can be described by the bulk GaN dispersion relationship multiplied by an effective medium constant (~ 0.65 for nanorod arrays without significant nanorod bundling such that a uniform effective medium model can be applied). Based on the optical measurements results, we propose a model to describe the light propagation within the nanorod array optical media and excellent numerical simulations of reflectivity spectra in the transparent region can be achieved using this model. Because of the superior material properties of GaN nanorods in terms of optical transparency, availability of *n*- and *p*-type conductivity, and excellent thermal and chemical stabilities, the reported results can have important implications for fundamental studies, as well as nanophotonics and optoelectronics applications.

Acknowledgments

This work is financially supported by the "Foresight Taiwan" program (NSC 96-3011-P-007-004) and the National Nanoscience and Nanotechnology Project (NSC 96-2120-M-007-008).